Pre-equilibrium and equilibrium emission of neutrons in ^{114}Cd(α,xn) reactions

J. Pal, S. Saha, C. C. Dey, P. Banerjee, S. Bose, B. K. Sinha, and M. B. Chatterjee
Saha Institute of Nuclear Physics, 1/AF Bidhanangar, Kolkata-700 064, India

S. K. Basu
Variable Energy Cyclotron Centre, 1/AF Bidhannagar, Kolkata-700 064, India
(Received 14 September 2004; published 22 March 2005)

The ^{114}Cd(α,xn) reaction has been studied for $E_\alpha = 35$–55 MeV following neutron emission and γ-ray deexcitation. Excitation functions of various (α,xn) channels measured from γ-ray yields have been compared with theoretical calculations based on ALICE-91 and CASCADE codes. Neutron energy spectra were generated from γ-gated neutron time of flight spectra. Neutron energy spectra corresponding to ($\alpha,3n$) and ($\alpha,4n$) reactions at $E_\alpha = 50$ MeV have been theoretically reproduced taking into account the contributions of equilibrated source with level density parameter $a = A/11$, along with the contributions from the pre-equilbrium process.

DOI: 10.1103/PhysRevC.71.034605 PACS number(s): 24.60.Dr, 24.60.Gv, 25.55.−e, 21.10.Ma

I. INTRODUCTION

Nuclear reactions induced by fast projectiles having energies above 10 MeV/A are governed by the strong interaction [1]. Under its influence, some fast particles are emitted before thermal equilibration. Fast projectiles incident on a target interact with the target nucleons and, as a result, energetic neutrons are predominantly emitted. Emission of energetic neutrons followed by nonstatistical γ rays arising out of particle-hole excitations are considered to be a pre-equilibrium process that occurs at the initial stage of the collision. At a later stage, with the formation of an equilibrated system of a compound nucleus, statistical evaporation of neutrons takes place.

A good deal of the nuclear reaction mechanism can be understood by examining the energy spectra of emitted neutrons [2–5]. In typical experiments, neutrons are detected in coincidence with the evaporation residues or fragments. Many of the gross features of the reaction mechanism, such as level density parameters, temperatures, and multiplicities, can be deduced from the inclusive and exclusive measurements of the neutron energy spectra. In reactions where many reaction channels are open, identification of the various channels through characteristic γ rays is utilized [6]. Thus, in (α,xn) reactions where the number of reaction channels are limited, selection of a particular residual channel can be made quite efficiently by detecting the characteristic γ rays.

Nuclear reactions induced by α particles of energies $\sim$30 MeV/A were studied earlier by Sakai *et al.* [7] on ^{164}Dy. It appeared from their studies of (α,xn) reactions that a considerable contribution of pre-equilibrium neutrons is observed in the forward direction, in addition to the contribution from the equilibrated compound nuclear system. As a result, one expects an interplay between the two reaction mechanisms, that is, the pre-equilibrium process and the compound nuclear process. Studies of heavy-ion-induced reactions on ^{158}Gd corroborate [8,9] the existence of both processes. However, studies on these aspects are rather rare and, therefore, further investigation is needed on other systems.

In the present work, ^{114}Cd(α,xn) reactions have been studied through (α,xn) channels by observing the γ rays and γ-gated neutrons corresponding to ($\alpha,3n$) and ($\alpha,4n$) channels with the motivation of observing the interplay of the two reaction mechanisms: pre-equilibrium and equilibrium processes at relatively low energy.

II. EXPERIMENTAL PROCEDURE

The experiment was carried out by bombarding an isotopically enriched (98.5%) target of ^{114}Cd (thickness $\approx$5.95 mg/cm^2) with α particles of energies 35–55 MeV from the Variable Energy Cyclotron at the VEC Centre, Calcutta. A schematic diagram of the experimental setup is shown in Fig. 1. The γ rays emitted from various reaction channels were detected with a large-volume HPGe detector (efficiency 25%) placed at an angle of 55° to the right side of the beam direction at a distance of 17 cm from the target, and the corresponding neutrons were detected with a 12.7-cm-diameter by 2.5-cm-thick NE213 detector (using a fast photomultiplier tube, Philips XP4512B). The neutron detector was placed at an angle of 50° to the left of the beam direction in two positions at distances of 50 and 100 cm from the target. The γ detector at a distance of 17 cm, and the neutron detector at a distance of 100 cm, subtended solid angles of 66.6 and 12.3 msr, respectively, at the center of the target. The standard slow-fast coincidence technique was used for the measurement of γ-gated neutrons. The spectra were recorded for accumulated charges of 6μC or more.

The contributions of scattered neutrons from the beam dump were reduced to a great extent by shielding the beam dump with paraffin blocks as well as with lead bricks. The HPGe detector was shielded from the background γ rays with lead bricks, and from the neutrons with borated paraffin. The neutron detector was shielded thoroughly with paraffin blocks from the scattered neutrons coming from the walls and roof of the experimental area and from other sources of neutrons such as slits and the beam pipe.

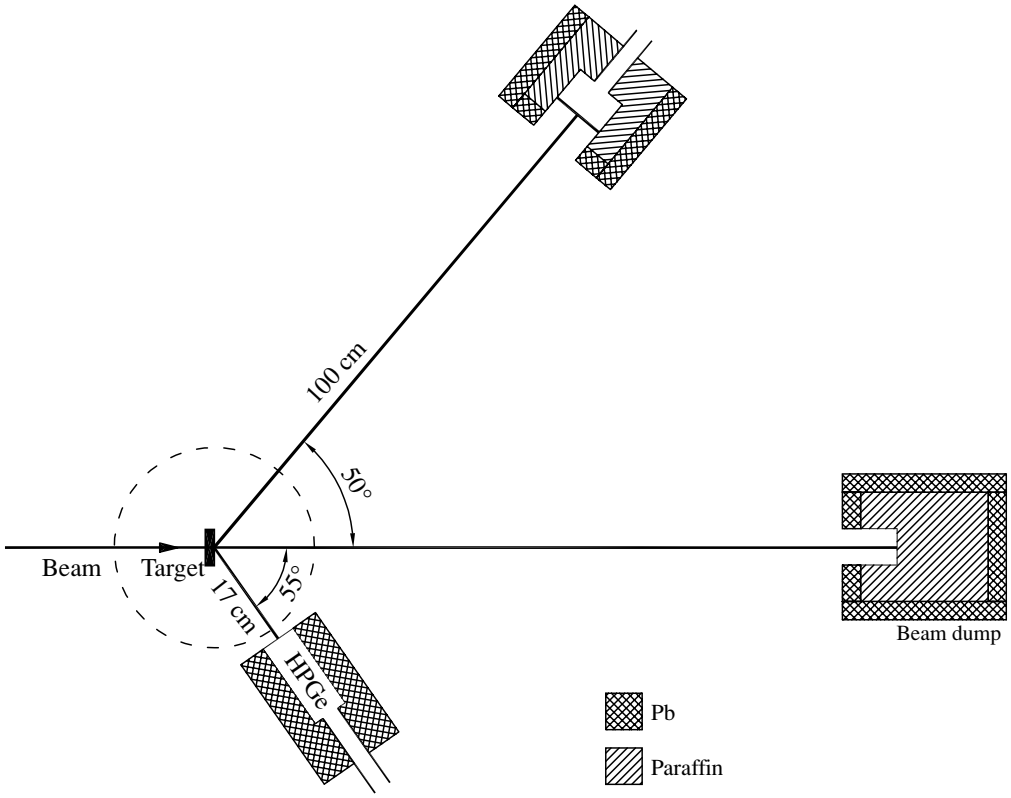

FIG. 1. A schematic diagram of the setup.

A pulse shape discriminator [10] was used for n-γ discrimination. Three-parameter list mode data were recorded with the ND computer facility of the VEC Centre. The time-of-flight (TOF) spectra of the emitted neutrons were recorded as follows: An event in the NE213 scintillator was used as the start signal for the TAC; the stop signal was then taken from the HPGe detector. The time period of the cyclotron beam bursts was ∼125 ns with a duration of ∼4 ns. With the use of a suitable delay and adjustment of the neutron flight path, neutron TOF was kept within the time period of two beam bursts (i.e., ∼125 ns). Time calibration of the system was done from the shift in the γ-γ prompt peak in the TAC spectrum, (a) with a change in the flight path and (b) with introduction of a fixed external delay in the stop channel of the TAC. A time delay of 0.8 ns per channel was set for the TAC. The time resolution of the HPGe-NE213 system was measured from the γ-γ prompt as 7.4 ns (FWHM). This time resolution was limited by the slow rise time of the pulses from the large HPGe detector. The time resolution of the NE213 detector was observed to be better than 1 ns measured separately with a coincidence setup between a BaF_2 detector and the NE213 detector.

Energy calibration of the NE213 detector was done with Compton edges of γ rays of ^{22}Na, ^{60}Co, and ^{137}Cs sources to determine the neutron energy threshold from the equivalent electron energy. In the present work, the neutron energy threshold for the NE213 detector was 1.06 MeV. The efficiency of the NE213 detector was calculated using the Monte Carlo simulation code MODEFF of Cecil *et al.* [11]. Single and coincidence spectra were analyzed using the computer program VECSORT. Neutron TOF spectra were generated by gating on the photo peaks of a number of selected γ rays of the various (α,xn) channels. Random contributions were obtained by generating the neutron TOF spectra with gates set around the photo peak of the same width as that of the photo peak and were subtracted to get the genuine coincidences. Typical neutron TOF spectra are shown in Fig. 2. The TOF spectrum shown in Fig. 2(a) contains all the γ rays detected with the HPGe detector and the correlated neutrons from various sources. A limited separation of neutrons and γ rays under such a condition is to be expected. The gated TOF spectra [Figs. 2(a) and 2(b)] with the gates set at characteristic γ rays of $(\alpha,3n)$ and $(\alpha,4n)$ processes show better n-γ separation.

A typical single γ-ray spectrum following the bombardment of an enriched ^{114}Cd target with α particles of energy $E_\alpha = 45$ MeV is shown in Fig. 3. The efficiency of the HPGe detector was calibrated with γ rays from ^{152}Eu and ^{60}Co sources of known strength and the intensities of the γ rays of interest were measured. To measure the evaporation residue (ER) cross sections $\sigma(\alpha, xn)$ of the various (α,xn) channels at different bombarding energies $E_\alpha = 35$–55 MeV, single γ-ray spectra were also recorded with the HPGe detector. In the measurement of overall error in cross section, the statistical error for the photo-peak area of γ rays, the error for the γ-ray efficiency of the detector (5%), the charge-measurement

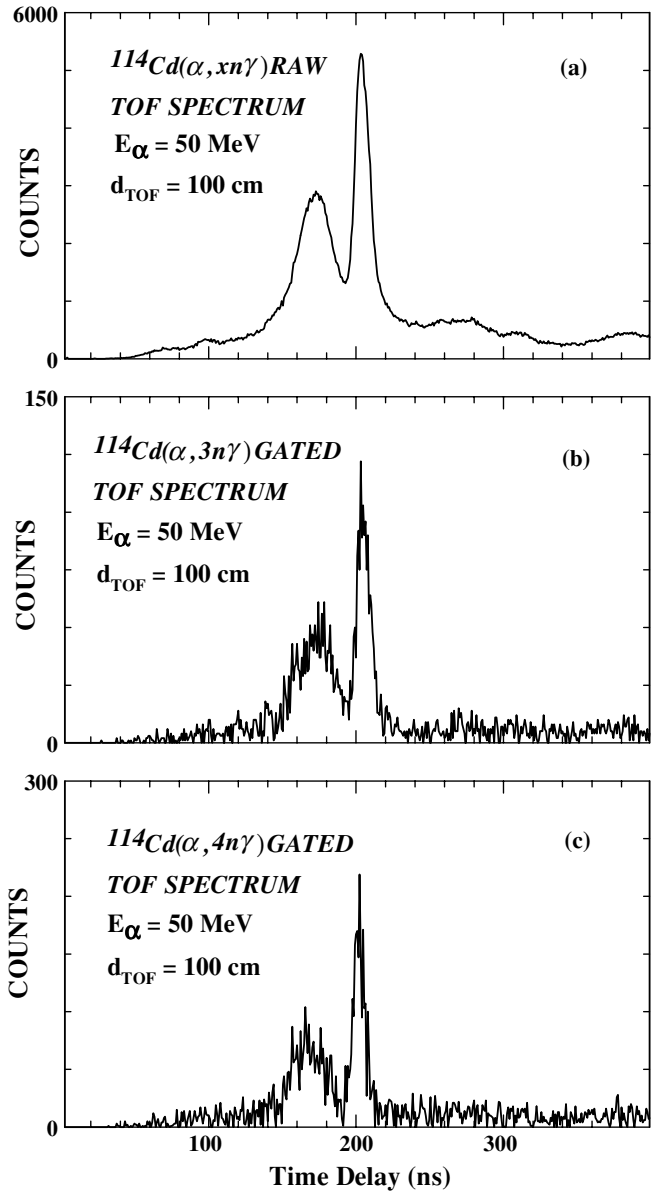

FIG. 2. γ-gated neutron time-of-flight spectra: (a) gate set for all γ rays, (b) gate set with γ rays of (α,3n) channel, (c) gate set with γ rays of (α,4n) channel.

error (2%), and the systematic error of fitting (3%) have been considered.

III. RESULTS AND DISCUSSION

The underlying mechanism of the excitation of a nuclear system at bombarding energy $E/A \sim$ a few MeV above the Coulomb barrier can be understood from the energy imparted to the target nucleus by the projectile. The overall excitation energy of the composite system is $E^* = E_{\rm cm} + Q$, where $E_{\rm cm}$ is the center-of-mass energy of the system and Q is the reaction Q value. Studies of neutron multiplicity could be a gauge to measure the excitation energy of the system since kinetic energy given to the system is not totally converted to excitation energy or heat. The average excitation energy of the system can thus be obtained from these studies provided the system has a negligible deformation. The nuclei in the vicinity of the proton shell closure at $Z = 50$ are nearly spherical and their energy spectra are vibrational in nature without significant deformation [12,13]. In the absence of deformation, E^* can be considered to be excitation energy of the system. Energy of the system is dissipated either by the emission of energetic particles (pre-equilibrium) or by particles evaporated from the equilibrated system. The main problem is the difficulty in separating the contributions of the two sources. However, the processes involved have two distinct features according to the underlying reaction mechanism. Depending on the time scale on which the neutrons are emitted, the possible sources are pre-equilibrium and equilibrium. Neutron evaporation from an equilibrated system occurs from a slowly moving compound nucleus on a larger time scale; neutron emission from a pre-equilibrium process, in contrast, occurs on a shorter time scale. The physical process of pre-equilibrium emission of neutrons is different from that of equilibrium emission. As a result, different angular correlations and energy spectra are observed in pre-equilibrium emission.

A. Identification of evaporation residues and measurement of cross section

The γ rays corresponding to the various xn channels can be identified easily from the γ-ray spectra observed at various bombarding energies. A typical γ-ray spectrum with the identification of γ rays corresponding to various evaporation channels is shown in Fig. 3. The spectrum is clean and similar spectra thus obtained at various α energies were used for the determination of ER cross sections of various xn channels. The excitation functions of the ^{114}Cd(α,xn) reaction have been measured using the characteristic γ rays of each (α,xn) channel. The maximum input angular momentum, brought into the compound nucleus by a 50-MeV α particle, is $l_{\rm max} \approx 25\hbar$ at an average excitation energy around 44 MeV. The average angular momentum of the compound nucleus, assuming uniform volume absorption, comes out to be $l_{\rm av} \approx 17\hbar$ [14]. The neutrons emitted from the compound nucleus populated the high-spin states of the residual nuclei. The decay modes of these states in residual nuclei are mainly through γ-ray transitions. It was observed earlier [15–19] that deexcitations of the nuclei occur mainly through ground-state transitions from the low-lying states and in even-even nuclei it occurs through $2^+ \rightarrow 0^+$ ground-state transitions. The transitions from the low-lying states can be used for studying the excitation functions of the (α,xn) channels. A similar method was applied earlier [19] for the measurement of excitation cross section of (α,xn) channels. The ER cross sections of Sn isotopes (^{113}Sn to ^{116}Sn) were obtained from the yields of the respective γ transitions considering their known branching ratios [15]. Since the contributions of the γ rays have been measured at 55° with the beam direction, the effect of angular distribution is insignificant because $P_2(\cos\theta)$ at this angle is zero. The transitions considered

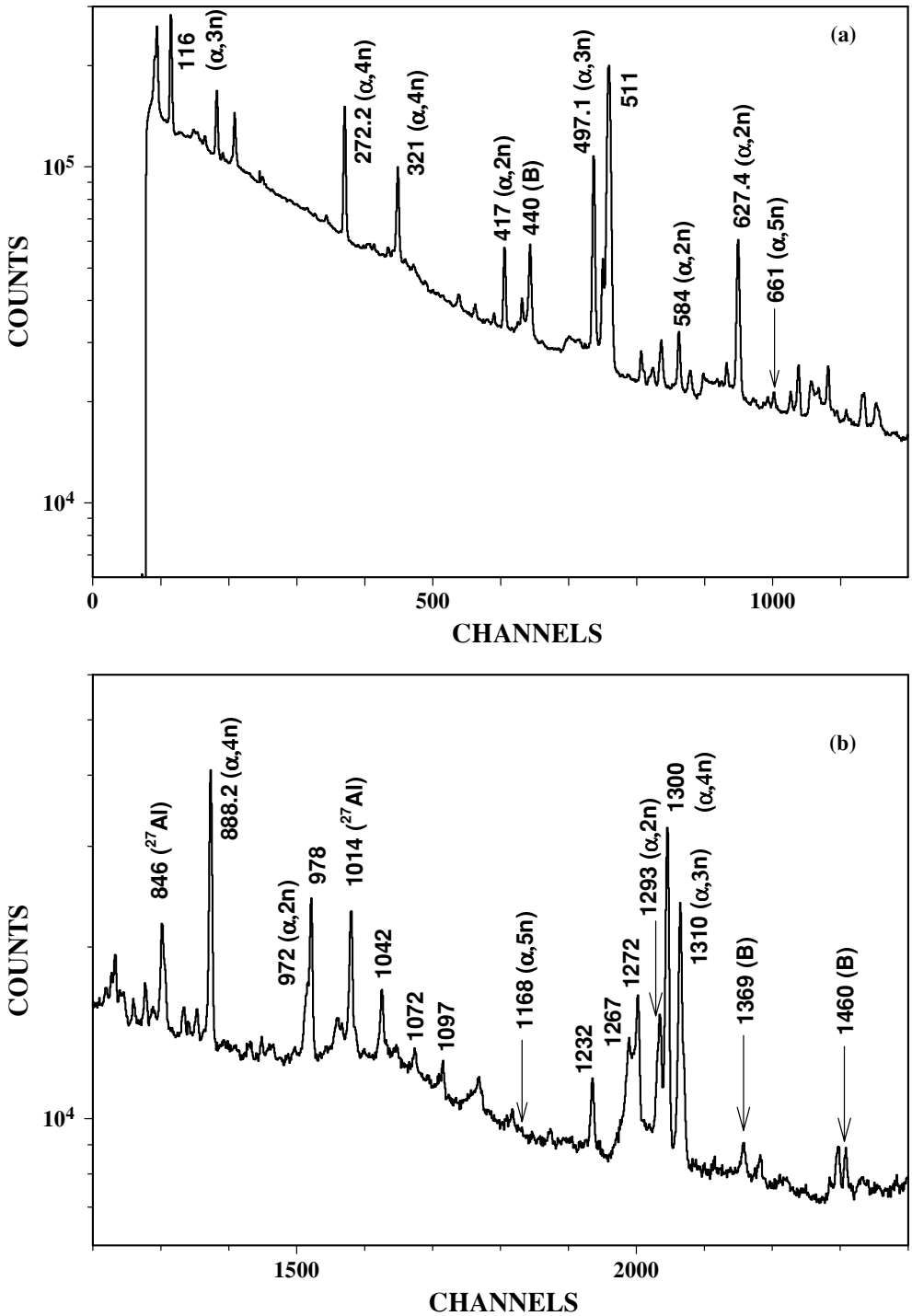

FIG. 3. γ-ray single spectrum taken with a 25% HPGe detector following the bombardment of an enriched ^{114}Cd target with 45-MeV α particles.

in the measurement of (α,xn) cross sections have already been assigned [15–19] as follows: 407.2 keV for $(\alpha,2n)$, 1310.0 keV for $(\alpha,3n)$, 888.2 and 1300.0 keV for $(\alpha,4n)$, and 661 and 1168 keV for $(\alpha,5n)$. Cross sections of other channels such as $(\alpha, ypxn)$ or $(\alpha,\alpha xn)$ are insignificant. No interfering γ rays from these processes are observed, as expected. Theoretical calculations [17] also corroborate these findings. The maximum contribution predicted from CASCADE for the $(\alpha,\alpha n)$ reaction is only 2.1 mb. The transitions that may have contributions from other channels or have contributions from contamination were discarded in measuring cross sections. A self-consistent method was applied for the normalization of the measured yields to the predicted cross sections on the basis of the ALICE-91 code [20] using the

TABLE I. Cross sections of ^{114}Cd(α,xn) reactions.

E_α(MeV)	Cross sections (mb)			
	$\sigma(\alpha,2n)$ 407 keV[a]	$\sigma(\alpha,3n)$ 1310 keV[a]	$\sigma(\alpha,4n)$ 888, 1300 keV[a]	$\sigma(\alpha,5n)$ 661, 1168 keV[a]
35	324 (26)2[b]	1166 (93)	31.5 (4.2)	—
40	161 (13)	1042 (83)	374 (32)	—
45	85.0 (6.9)	539 (43)	927 (76)	—
50	48.6 (3.9)	223 (18)	1340 (108)	49.2 (5.0)
55	26.1 (2.5)	112 (11)	811 (66)	191 (18)

[a]Transitions considered.

[b]Numbers in parentheses denote errors over cross-section measurement.

level density formula of Kataria *et al*. [21]. Cross sections determined for various (α,xn) channels are shown in Table I. The cross sections are compared with the predicted values obtained from ALICE and CASCADE [22] codes and are shown in Fig. 4. It has been observed that the values are reproduced very well from calculations based on the ALICE code. It appears from Fig. 4 that calculations based on the CASCADE code underpredict (α,$2n$) cross sections and overpredict (α,$5n$) cross sections whereas (α,$3n$) and (α,$4n$) cross sections are reproduced reasonably well.

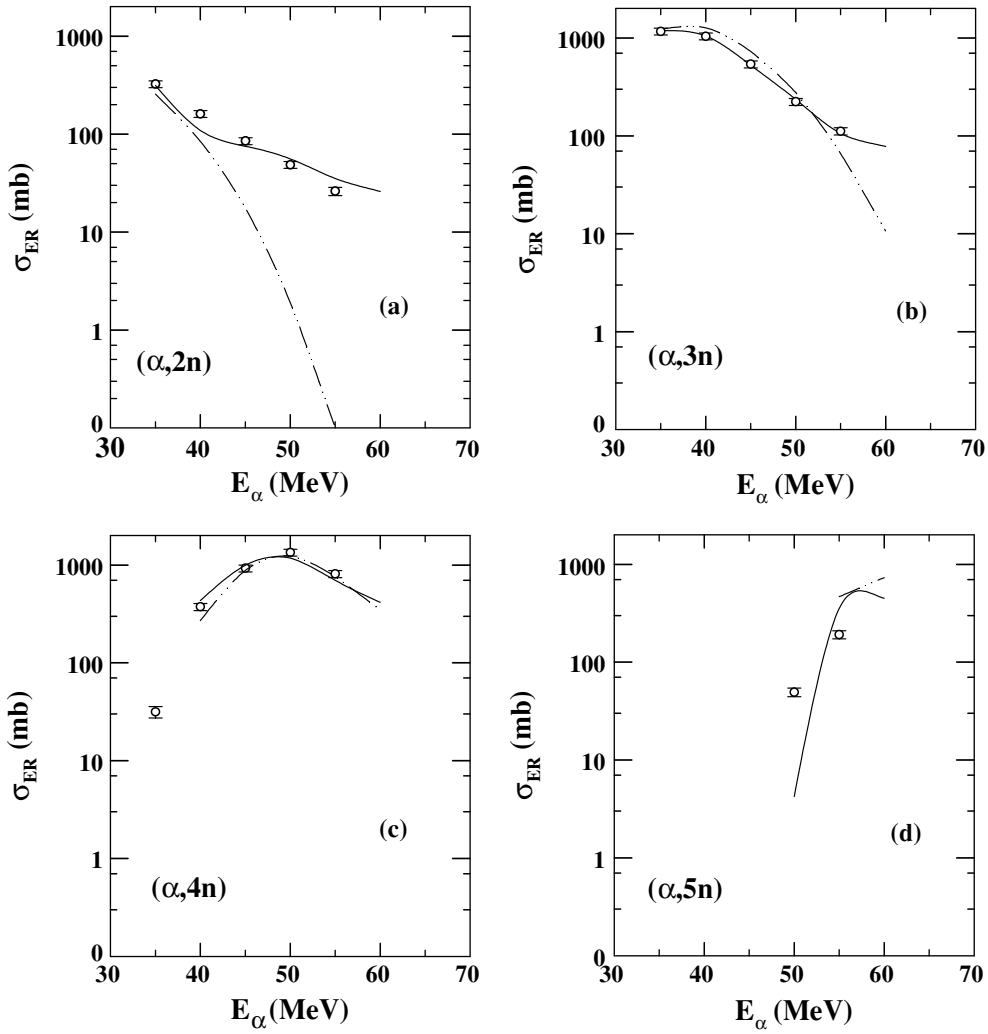

FIG. 4. Comparison of cross sections of various ^{114}Cd(α,xn) channels with the theoretical calculations based on ALICE and CASCADE codes. Experimental data points (o), ALICE calculations for compound process (solid line), and CASCADE calculations (dot-dashed line) are shown.

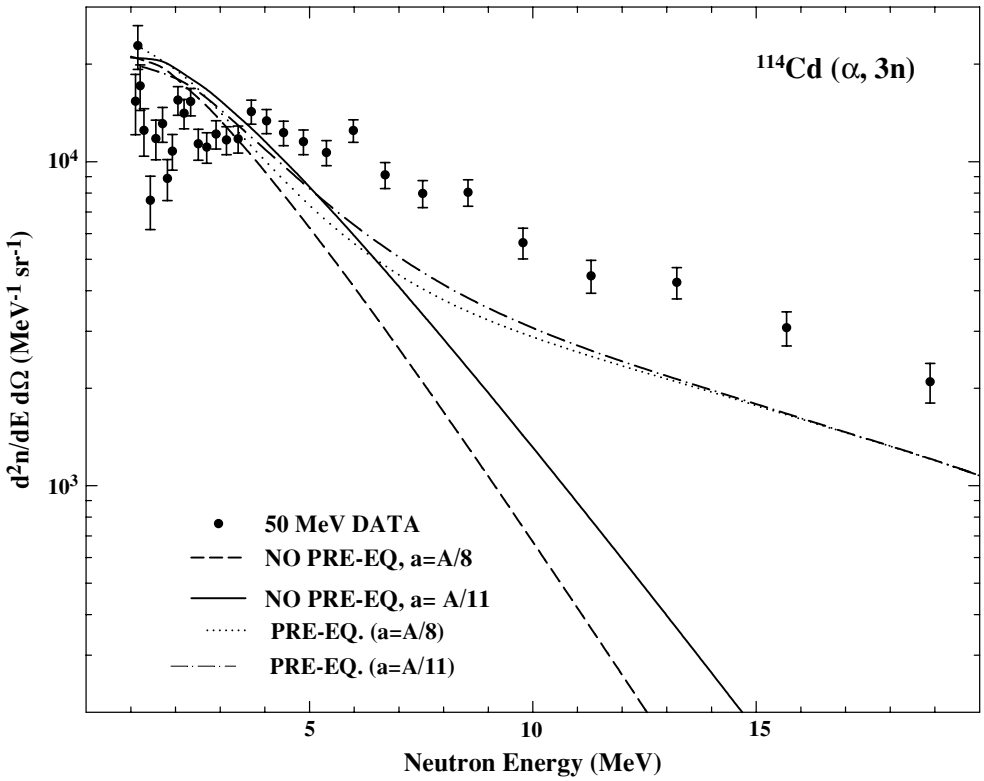

FIG. 5. Neutron energy spectrum corresponding to the $(\alpha,3n)$ channel at $E_\alpha = 50$ MeV. Also shown are the theoretical predictions based on an ALICE calculation assuming emission from a compound system with level density parameter $a = A/8$ (solid line) and $a = A/11$ (dashed line) and assuming emission from a compound plus precompound system with $a = A/8$ (dotted line) and $a = A/11$ (dot-dashed line).

B. Interpretation of neutron energy spectra and determination of level density parameter

It was shown earlier [14] in the ^{209}Bi(α,xn) reaction at energies of 34 and 52 MeV that incorporation of pre-equilibrium neutron emission was needed to explain the spin saturation effect of the excited states of the residual nuclei at an energy of 52 MeV. In our earlier studies [19] of the ^{116}Cd(α,xn) reaction, we also observed such a spin saturation effect. The present work on ^{114}Cd(α,xn) done in the same energy domain is expected to show a similar behavior. The γ-gated neutron TOF spectra corresponding to $(\alpha,3n)$ and $(\alpha,4n)$ channels were converted to the neutron emission spectra taking neutron detection efficiency [11] into consideration. The spectra corresponding to $(\alpha,3n)$ and $(\alpha,4n)$ channels are shown in Figs. 5 and 6, respectively. A cursory inspection of the neutron spectra shows that neutron energies are distributed with significant yield over a wide range in both these spectra. It is known [2] that the emission of particles from a thermalized system is isotropic in the rest frame of the emitter and that the emitted particles have Maxwellian velocity distribution. It has been demonstrated [23] experimentally that the double differential multiplicity distributions of the emitted neutrons from an evaporated cascade in the laboratory frame can be expressed as

$$\frac{d^2n}{dEd\Omega} = \frac{n}{2(\pi T)^{3/2}}\sqrt{E}\exp[-(E - 2\sqrt{\epsilon E}\cos\theta_n + \epsilon)/T],$$

where E is the neutron energy in laboratory frame, n is the neutron multiplicity, T is the temperature of the nucleus, θ_n is the angle of emission of the neutrons with the emitting nucleus, and ϵ is the laboratory energy per particle of the recoiling nucleus. The recoil velocity of the compound nucleus is $\sim$0.17 cm/ns and emission of neutrons from a source moving with such a low velocity is inadequate to explain the high-energy tail of the neutron energy spectra.

The ALICE calculation [20] has been done with exciton number $n_o = 4$ using two level density parameters, $A/8$ and $A/11$. The calculation considering emission only from the compound system could not reproduce the neutron energy spectra. The simulation with level density parameter $a = A/11$ has reproduced the neutron energy spectra satisfactorily compared to that with $a = A/8$ but only up to 5 MeV. Neutron energy spectra beyond 5 MeV show the presence of high-energy neutrons. As stated earlier, evidence of pre-equilibrium neutron emission has been reported [14] in (α,xn) reactions at this energy. According to the Fermi JET or PEP (promptly emitted particles) model [24], neutrons would be highly energetic depending on the kinematics of the incident projectile. These neutrons are emitted preferentially in the direction of the linear momentum transfer (i.e., forward direction). A similar feature is also observed in the present work. Hence, for the interpretation of neutron energy spectra, the ALICE calculation was done with inclusion of precompound emission and neutron energy beyond 5 MeV could be reproduced quite

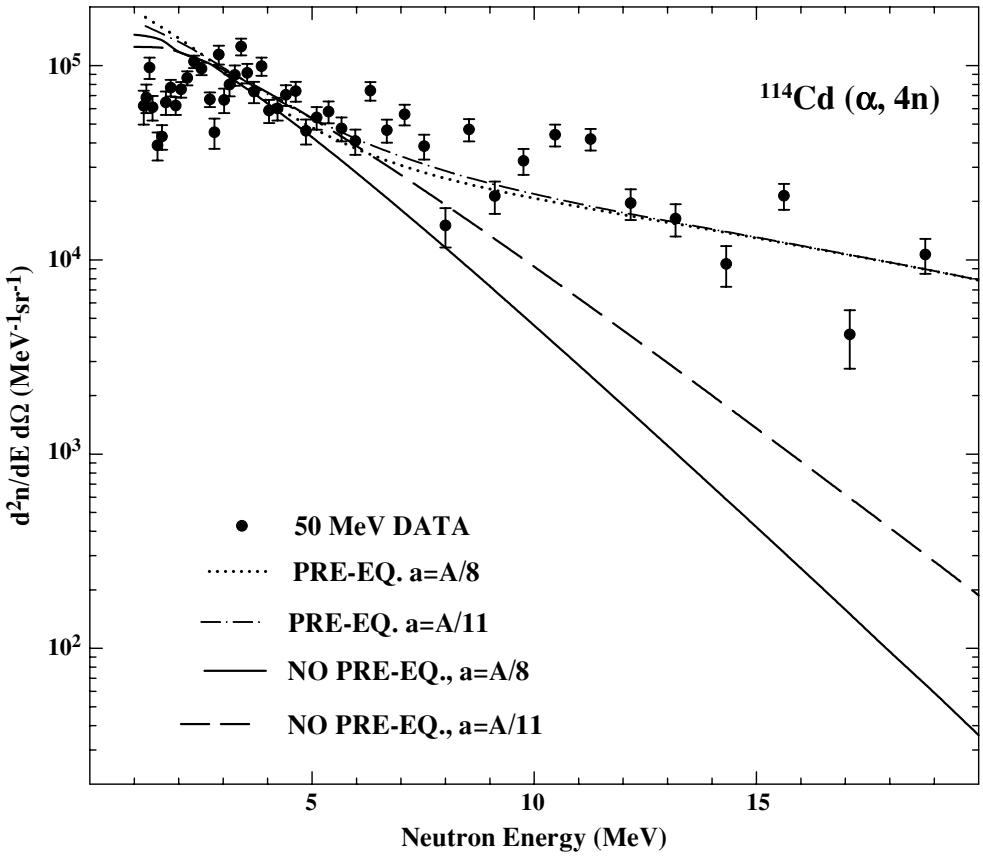

FIG. 6. Neutron energy spectrum corresponding to the $(\alpha,4n)$ channel at $E_\alpha = 50$ MeV. Also shown are the theoretical predictions based on an ALICE calculation assuming emission from a compound system with level density parameter $a = A/8$ (solid line) and $a = A/11$ (dashed line) and assuming emission from a compound plus precompound system with $a = A/8$ (dotted line) and $a = A/11$ (dot-dashed line).

well for the $(\alpha,4n)$ process, as shown in Fig. 6. However, the pre-equilibrium part of the neutron energy spectrum of the $(\alpha,3n)$ process could not be reproduced well (Fig. 5). The ALICE calculation underpredicts the yield in magnitude by 20–50% in the energy range of 5–20 MeV. It may be pointed out that different parameters of the moving source (velocity and slope parameter) are needed to explain the pre-equilibrium spectra corresponding to different evaporation residues [25]. This may be the reason for the failure of ALICE to predict the high-energy part of the neutron spectrum corresponding to the $(\alpha, 3n)$ process. A better fit to the low-energy parts of the neutron spectra with level density parameter $A/11$ in this mass region around $T = 2.2$ MeV is in good agreement with the reported values [26–28] and with the theoretical prediction of Shlomo and Natowitz [29].

The dominant reaction channel $(\alpha, 4n)$ at $E_\alpha = 50$ MeV is well reproduced with the calculations from the ALICE code with inclusion of pre-equilibrium neutrons (Fig. 6). It may be concluded that studies of γ-ray spectra following the (α,xn) reactions, which are analogous to isotopic tagging, can be utilized for the measurement of ER cross sections. From comparison of predicted values of cross sections, it appears that the calculation with ALICE described the reaction mechanism in ^{114}Cd(α,xn) reaction at $E_\alpha = 35-55$ MeV quite well. The γ-gated neutron TOF studies have been successfully used in understanding the pre-equilibrium and equilibrium (compound nuclear) processes. Important parameters, including level density or average excitation energy, can be extracted from such studies.

ACKNOWLEDGMENTS

We are grateful to Dr. J. Galin of GANIL for stimulating discussions and valuable suggestions that have improved the quality of the paper. We thank the cyclotron operators of the VEC Centre for smooth running of the accelerator. Thanks are due to Ms. Sarmishtha Bhattacharya of the VEC Centre for her help during the experiment.

[1] M. Blann, Phys. Rev. C **31**, 1245 (1985).
[2] W. U. Schröder and J. R. Huizenga, in *Treatise on Heavy-Ion Science*, edited by D. A. Bromley (Plenum, New York, 1984), Vol. 2, Chap. 3, p. 133.
[3] D. J. Hinde *et al*., Phys. Rev. C **45**, 1229 (1992).
[4] M. B. Chatterjee *et al*., Phys. Rev. C **44**, 2249 (1991).
[5] L. Fiore *et al*., Phys. Rev. C **50**, 1709 (1994).
[6] R. Palit *et al*., Nucl. Instrum. Methods A **443**, 386 (2000).

[7] H. Sakai, H. Ejiri, T. Shibata, Y. Nagai, and K. Okada, Phys. Rev. C **20**, 464 (1979).
[8] D. G. Sarantites, L. Westerberg, M. L. Halbert, R. A. Dayras, D. C. Hensley, and J. H. Barkar, Phys. Rev. C **18**, 774 (1978).
[9] L. Westerbeg, D. G. Sarantites, D. C. Hensley, R. A. Dayras, M. L. Halbert, and J. H. Baker, Phys. Rev. C **18**, 796 (1978).
[10] S. Bose, M. B. Chatterjee, B. K. Sinha, and R. Bhattacharya, Nucl. Instrum. Methods A **270**, 487 (1988).
[11] R. A. Cecil, B. D. Anderson, and R. Madey, Nucl. Instrum. Methods **161**, 439 (1979).
[12] W. T. Milner, P. K. McGowan, P. H. Stelson, R. L. Robinson, and R. O. Sayer, Nucl. Phys. **A129**, 687 (1969).
[13] Z. W. Grabowski and R. L. Robinson, Nucl. Phys. **A206**, 633 (1973).
[14] P. Mukherjee, I . Mukherjee, P. Sen, and C. Samanta, Phys. Rev. C **36**, 1197 (1987).
[15] J. Blachot and G. Marguier, Nucl. Data Sheets **75**, 739 (1995).
[16] J. Blachot, Nucl. Data Sheets **59**, 729 (1990).
[17] J. Blachot and G. Marguier, Nucl. Data Sheets **67**, 1 (1992).
[18] A. Van Poelgeest, J. Bron, W. H. A. Hassellink, K. Allaart, J. J. A. Zalmstra, M. J. Uitzinger, and H. Verheul, Nucl. Phys. **A346**, 70 (1980).
[19] M. B. Chatterjee, P. Banerjee, B. K. Sinha, S. Bose, R. Bhattacharya, and S. K. Basu, Phys. Rev. C **42**, 2737 (1990).
[20] M. Blann, NEA Data Bank, Gif-sur-Yvette, France, Report No. PSR-146, 1991.
[21] S. K. Kataria, V. S. Ramamurthy, and S. S. Kapoor, Phys. Rev. C **18**, 549 (1978).
[22] F. Puhlhofer, Nucl. Phys. **A280**, 267 (1977).
[23] D. Hilscher *et al*., Phys. Rev. C **20**, 556 (1979).
[24] J. P. Bondorf, J. Phys. C **5**, 195 (1976).
[25] J. P. Coffin, in *Frontiers of Heavy-Ion Physics*, edited by N. Cindro, W. Greiner, and R. Caplar (World Scientific, Singapore, 1987), p. 227.
[26] R. Wada *et al*., Phys. Rev. C **39**, 497 (1989).
[27] A. Chbihi *et al*., Phys. Rev. C **43**, 666 (1991).
[28] J. L. Wile *et al*., Phys. Rev. C **51**, 1693 (1995).
[29] S. Shlomo and J. B. Natowitz, Phys. Rev. C **44**, 2878 (1991).